

Investment of Cyclic Prefix to Reduce the Peak-to-Average Power Ratio and Recover Original Phases Blindly

Mohammed I. Al-Rayif

Original scientific article

Abstract—When dealing with the phenomenon of unexpected high peak-to-average power ratio (PAPR) caused by multicarrier techniques, it is rarely to find a proposed solution that addresses the most important challenges together, that are; reducing the PAPR, achieving performance identical, mostly, to the theoretical curve and a reasonable level of computational complexity. This paper presents a new proposal that is able to achieve these three criteria together as the following. First, reducing the PAPR curves through easy development in the selective mapping (SLM) structure. Second, identifying the original transmitted phase block by taking advantage of the cyclic prefix structure and its mechanism, without any explicit side information, while maintaining the system performance. Lastly, these achievements were obtained at low computational complexity comparing to the traditional methods of SLM PAPR reduction schemes. This proposed method is referred to as; Injected and Extracted Short-SLM to and from the Cyclic Prefix (IES-SLM-CP). The appropriate short phase sub-block is injected to a specific locations of CP, and at the receiver side, this sub-block can be extracted from the CP to reconstruct the whole original phase block.

Index Terms—Cyclic Prefix, Selective mapping, Peak-to-Average Power Ratio, Non-Linear High-Power Amplifier.

I. INTRODUCTION

WHEN reducing an orthogonal frequency division multiplexing peak-to-average power ratio (OFDM-PAPR) to a certain level, via a specific method, it is necessary to maintain both bit error rate (BER) performance and computational complexity around an acceptable levels. Achieving these three factors together (Low PAPR, low BER, and low computational complexity), undoubtedly, is a real challenge for the developer. To satisfy these thresholds, a huge number of researches have been represented, such as, for instance, the distortionless methods (i.e. selective mapping (SLM) and partial transmit sequences (PTS) families) [1], [2], [3], companding techniques [4], encoding family schemes[5], tone reservation (TR) methods [6], clipping and filtering schemes [7], [8], artificial neural networks (ANN) family [9] and, recently, the chaotic sequences family [10]. This section, however, will discuss the recent proposals and those which were, in somehow, able

to achieve the three factors together (Low PAPR, low BER, and low computational complexity), especially since this study satisfies all these factors, proportionally. Besides, this proposal will focus on studies that use distortionless methods such as SLM within the cyclic prefix (CP), where is applicable, which have been relied upon in the construction of this proposal. Accordingly, based on the survey, Valluri, S. P. *et al.* [2] provided a simple side information (SI) cancellation algorithm using pilots associated with channel estimation in the presence of DC-biased optical orthogonal frequency division multiplexing (DCO-OFDM) system. Moreover, Al-Rayif M. I. *et al.* [12] represented a novel PAPR reduction technique in the transmitter DSP of a fiber mobile fronthaul network, named as iterative selective mapping (I-SLM). The proposed algorithm uses orthogonal phase vectors construction to reduce the level of PAPR while recognizing the desired original phase sequence is recovered without explicit SI. Thota S. *et al.* [13] discussed a hybrid method, where the SLM was combined with PTS, and PTS/SLM techniques were combined with companding methods (μ -low and A -low) to analyze its characteristics in terms of PAPR and BER. In addition to that, probabilistic schemes participated in reducing PAPR in the presence of UFMC (as a multi-carrier system) like [11], [1]. The Dcomp-SLM represented by Al-Rayif M. *et al.* [11] is capable to reduce PAPR while maintaining the PSD and BER of the OFDM signal by separating real and imaginary components of the base-band frames for PAPR reduction process. While the proposal of Fathy, S. A. *et al.* [1] provided a modified SLM (P-SLM) approach to utilize the linearity property of the UFMC modulator, while an alternative $\sqrt{U_w}$ UFMC waveforms were considered to reduce PAPR. Furthermore, Hou, J. *et al.* [14] introduced a multi-objective quantum inspired evolutionary SLM scheme to resolve the PAPR combinatorial optimization problem. Besides that Liang, H. [15] achieved a PAPR reduction by implementing the structure of Reed-Muller codes to set an adaptive threshold value to evaluate the characteristics of input signals and select the optimal produced phase sequences. On the other side, the PTS technique is employed, by Al-Jawhar, Y. A. *et al.* [3], to reduce the high PAPR value of an filtered OFDM (F-OFDM) system. Also, SLM scheme was employed in Multicarrier Faster-Than-Nyquist (MFTN) technique, to reduce its high PAPR, by Cai, B. *et al.* [16]. Recently, SLM scheme was applied to serve the information security as well as PAPR

Manuscript received September 9, 2022; revised October 24, 2022. Date of publication November 24, 2022. Date of current version November 24, 2022. The associate editor prof. Gordan Šišul has been coordinating the review of this manuscript and approved it for publication.

M. I. Al-Rayif is with the King Saud University, Electrical of Applied Engineering Department, P. O. BOX 2454, Riyadh 11451, Saudi Arabia, e-mail: malrayif@ksu.edu.sa.

Digital Object Identifier (DOI): 10.24138/jcomss-2022-0115

reduction such as, for example, the proposal of Haroun, M. F. and Gulliver, t. A. [17]. They represented a PAPR reduction while securing the transmitted OFDM signal via generating a random chaotic sequences using Selective Mapping (SLM) technique. This method depends on the dynamics of the logistic map which are described by the difference equation $x_{n+1} = rx_n(1 - x_n)$, where the state variable x_i is a number between zero and one. The parameter r can be given any value of the region $3.56995 \leq r < 4$. Here, multiple phase sequences were generated from this logistic map equation and, then, used it to modify the original phases of the OFDM sequence. This concept helps to improve the PAPR while maintaining the performance of BER. Nevertheless a high computational complexity was introduced due to implementing FFT and quantization operations on the chaotic sequence, besides to the complexity which has been obtained during the SLM scheme and IFFT operations. Moreover, Simsir, S. and Taspinar, N. [18] provided the directed cuckoo search selective mapping (DCS-SLM) algorithm to minimize the PAPR in the presence of OFDM-UFMC scheme. This method introduced an algorithm that modifies the maximum OFDM peaks by flipping the generated random phases; hence, the extra PAPR reduction can be achieved, but at the expense of the orthogonality of the OFDM system. Also, this proposal required high computational complexity at many stages of the processing. For instance, the IFFT process is implemented for each candidate phase sequence c , for $1 \leq c \leq C$, and the square absolute value is accounted for each OFDM subcarrier n , for $1 \leq n \leq N$, to identify the maximum peak. This is besides the rest of operations for the provided algorithm steps, UFMC, and FFT and recovery processes, which act as an extra computational complexity.

Despite the previous discussed proposals, various mechanisms of PAPR reduction have been shown for different types of multicarrier technology (OFDM, F-OFDM, UFMC, ... etc) over a wireless and optical networks, yet none of them offer PAPR reduction by utilizing the cyclic prefix part as in this study. To the best of our knowledge, there is no proposal that provided the same method as presented in this study except for the research represented by [19], where the cyclic prefix (CP) is used in optical system for the purpose of data encryption mechanism. Briefly, they demonstrated that the current OFDM frame $s[n]$ is used to produce encryption keys to encrypt and decrypt the next generation OFDM frame $s[n+1]$. In the proposed method, however, a very short random phase sequence, among U phase sequences. The one which introduces the lowest PAPR is considered for transmission and its short copy is modified by a certain decision metric, then inserted at a specific location inside the cyclic prefix (CP). At the recovery stage, a short equalizer is implemented to rebuild the short phase sequence blindly to recover the OFDM frame to its original phase sequence. In our proposal, satisfying performances of both BER and PAPR are obtained while the computational complexity is remarkable, as will be demonstrated in the following sections.

The reminder of the paper is organized as follows. The proposed system model is provided in the Section II, followed by the simulation results and discussions in Section III. Finally,

in Section IV, some concluding remarks are provided.

Notation: sub-vectors/vectors, sub-blocks/blocks, sub-frames/frames and matrices are boldface small and capital letters; the transpose, complex conjugate and inverse of matrix \mathbf{A} are denoted by \mathbf{A}^T , \mathbf{A}^* , \mathbf{A}^{-1} , respectively; k, n, u , and v indicate the indices of a sequence in frequency domain, time domain, the candidate phase vector, and the desired phase vector, respectively; $|\cdot|$ and $\mathbf{E}\{\cdot\}$ denotes the norm value(amplitude) and statistical expectation, respectively.

II. PROPOSED SYSTEM MODEL

In the proposed method, for simplicity, the SLM non distortion (probabilistic) technique is simulated with a specific modification in its construction to fit in the proposed concept, however any other distortionless scheme can be used instead as long as the conditions of the proposal are considered.

A. OFDM System with SLM Scheme

Assume a typical SISO-OFDM system with N subcarriers, as shown in Fig.1. The OFDM system takes a set of input data bits stream $\mathbf{a} = [\mathbf{a}_0, \mathbf{a}_1, \dots, \mathbf{a}_{(N-1)}]$, where $\mathbf{a}_i = [a_{i1}, a_{i2}, \dots, a_{i(\log_2 M)}]$ is a bit sub-stream, which are modeled using M -QAM to map onto the complex channel base-band symbol $\mathbf{X}_k = [X_0, X_1, \dots, X_{N-1}]^T$, where $0 \leq k \leq N-1$ and $[\cdot]^T$ is the transpose operation. Such modulated symbols N are packed together to form $N \times 1$ parallel complex symbols. Simultaneously, each complex symbol X_k is multiplied with the corresponding element of the random candidate phase element $p_k^u \forall u \in \{0, 1, \dots, U-1\}$, where U is the overall generated phase blocks and $p_k^u \in \{-1, 1\}$, as will be represented in the next subsection. An inverse fast Fourier transform (IFFT) is applied for each modified U frames, in addition to the IFFT of the original complex data symbols X_k . Where the IFFT function can be expressed as follows:

$$x_n = \frac{1}{N} \sum_{k=0}^{N-1} X_k e^{i2\pi \frac{kn}{N}}, \quad (1)$$

where $n \in \{0, 1, \dots, N-1\}$. Hereafter, the peak-to-average-power ratio (PAPR) is accounted for each OFDM outcome signal as follows:

$$PAPR = \frac{\max_n [|x_n|^2]}{E [|x_n|^2]}. \quad (2)$$

The characteristic of the proposed PAPR reduction is evaluated by determining the CCDF of the lowest $PAPR_{u^*}$ obtained for an OFDM frame of (2) for $U+1$ OFDM block copies, where $CCDF_{PAPR} = P_r \{PAPR > PAPR_{threshold}\}$ and it will be discussed deeply in subsection (III-A), taking into account that the extra one indicates the original OFDM symbol. Consequently, the u -th OFDM symbol with the minimum PAPR, \mathbf{x}^u , is considered for transmission, that is

$$\mathbf{x}^v = \mathbf{x}^u \left\{ \arg \min_{0 \leq u \leq U} [PAPR^u] \right\}. \quad (3)$$

Noting that the over sampling factor is applied, in this proposed method, with value of 4, to make the CCDF-PAPR

derived performance valid. From this point onward, and for simplicity, this factor will not be indicated in the following equations.

B. Proposed SLM Design and Recovery Blindly

In this section we will demonstrate the proposed method of generating, storing and recovering the desired phase vector \mathbf{P}^v , where $v \in [0, 1, \dots, U-1]$, without the need to explicitly its side information nor the matrix of the candidate phase vectors \mathbf{P} . Consequently, a phase sub-vector $\mathbf{P}^{u,D}$ is generated randomly with length $D \ll N_c$ where $\mathbf{P}^{u,d} = [p^{u,0}, p^{u,1}, p^{u,2}, \dots, p^{u,D-1}]$, $\forall u \in \{0, 1, 2, \dots, U-1\}$ and N_c is the length of cyclic prefix sequence. Each generated phase sub-vector is repeated $\frac{N}{D} + N \bmod D$ to match the length N of the data block (Noting that the values of D is selected in this proposal such that the remainder $N \bmod D = 0$). Hence, at the end, the designed u th phase vector can be expressed as;

$$\mathbf{P}^u = \left[\underbrace{\overbrace{p^{u,0}, p^{u,1}, \dots, p^{u,D-1}}^{\mathbf{P}^{u,D}}}_{0}, \dots, \underbrace{p^{u,0}, p^{u,1}, \dots, p^{u,D-1}}_{N-1} \right]. \quad (4)$$

Same processes are applied to generate the library of U phase vectors to be used prior to the IFFT operation by multiplying each element in u th candidate phase block \mathbf{P}^u with the corresponding data symbol \mathbf{X} as described in the last subsection. After the IFFT operation, for all $U+1$ copies of \mathbf{x}^u , the PAPR _{u} is calculated, including the original PAPR for which no phases modifications were applied to the original data sequence, i.e. $U+1$ different values of the PAPR are countable. Last but not least, the OFDM symbol \mathbf{x}^v which introduces the lowest PAPR will be transmitted. For the process of recovering the original phase sequence blindly at the receiver, the cyclic prefix (CP) period has been invested by injecting the desired phase sub-vector $\mathbf{P}^{v,D}$ inside it at a specific short location. A certain threshold $\alpha = \beta + j\gamma$ is replaced, instead, at only the correspondence positive ones of the sub-vector $\mathbf{P}^{v,D}$, while the negative ones are unchangeable (in this proposal $\beta = \gamma = \mathbf{E}\{|x[n]|\}$). The purpose of this modification is to rebuild the elements of the transmitted phase sub-vector $\mathbf{P}^{v,D}$ at the receiver, and to identify, in turn, the whole elements of the vector \mathbf{P}^v without the need to store the candidate phase matrix. As a result, a comparable level of computational complexity is achieved. To expound the concept of investing CP for the benefit of the proposal, let us review the mechanism of CP operation. As is well known that the CP is added to the beginning of the time domain OFDM block to protect it from the effects of inter-symbol-interference (ISI) and inter-carrier-interference (ICI) resulted from the multipath fading channel [21]. Depending on the definition of the distribution of the Rayleigh fading channel, the assumption of large number of randomly phased components, and the central limit theorem, the generated channel can be modeled as a complex Gaussian realization. Hence, the magnitude of the generated channel (envelope) performs as the same as the distribution of Rayleigh probability density function (pdf), considering that the channel mean value equals to zero [22], [23]. On this basis, it can be

observed that the most impact of the channel is concentrated around the variance of channel distribution. In other words, the deep channel fading effect will, mostly, appear in the front of the cyclic prefix, while the superficial channel effect is extended to the tail of the cyclic prefix. Therefore, the effect of multipath fading channel can be resolved at the stage of getting rid of the CP at the receiver side. From this standpoint, the transmitted phase sub-block $\mathbf{P}^{v,D}$ is injected in CP period within this duration which can be reconstructed at the stage of removing channel effect, as depicted in Fig.2, assuming the length of CP is $N_c = \frac{N}{4}$ where $N_c \gg L$ and L is the maximum number of fading channel paths, where the channel in the proposed method has been considered to be known perfectly at the receiver. It should be noticed that the location and length of injected phase sub-block will impact on the system performance. For instance, in the case when considering the CP tail for injecting the phase sub-block, it means that the impact of the channel fading will reach the injected phase sub-block, leading to side information distortion and high data bit error rate, which indicates that the condition $N_c \gg L$ has become useless. Analytically, let the equivalent discrete-time complex received signal at index n is expressed as

$$r[n] = h[n] * x[n] + z[n] = \sum_{l=0}^{L-1} h[n] \cdot x[n-l] + z[n], \quad (5)$$

where, $n \in \{-N_c, -N_c+1, \dots, 0, 1, \dots, N-1\}$, $(*)$ denotes the convolution operation, and $z[n]$ is the additive white Gaussian noise (AWGN) with zero mean value and variance σ_n^2 , at index n . Equivalently, in the matrix form, (5) can be formulated as $\mathbf{r} = \mathbf{h} * \mathbf{x} + \mathbf{z}$, where;

$$\mathbf{r} \triangleq \begin{bmatrix} r_1 \\ r_2 \\ \vdots \\ r_{(N+N_c-L+1)} \end{bmatrix}, \mathbf{x} \triangleq \begin{bmatrix} x_1 \\ x_2 \\ \vdots \\ x_{N+N_c} \end{bmatrix}, \mathbf{z} \triangleq \begin{bmatrix} z_1 \\ z_2 \\ \vdots \\ z_{(N+N_c+L-1)} \end{bmatrix}, \quad (6)$$

While the channel vector \mathbf{h} is

$$\mathbf{h} \triangleq \begin{bmatrix} h_0 \\ h_1 \\ \vdots \\ h_{(L-1)} \end{bmatrix}. \quad (7)$$

The zero forcing linear equalizer is implemented to detect the desired phase sub-block $\mathbf{P}^{v,D}$. Hence, the $(N+N_c+L-1) \times (N+N_c)$ down-shift columns of the transpose channel matrix can be expressed as

$$\mathbf{h}' \triangleq \begin{bmatrix} h_0 & h_1 & \dots & h_{L-1} & 0 & \dots & 0 \\ 0 & h_0 & \dots & h_{L-2} & h_{L-1} & \dots & 0 \\ \vdots & & \ddots & & & & \\ 0 & \dots & & h_0 & \dots & h_{L-2} & h_{L-1} \end{bmatrix}, \quad (8)$$

Assuming $\mathbf{H} = [\mathbf{h}']^T$, accordingly, the ZF equalizer is $\mathbf{g}^{ZF} = \mathbf{H}[\mathbf{H}^H \mathbf{H}]^{-1}$, where $(\cdot)^H$ represents the complex conjugate transpose [24]. Note that the range of interest, in this process, is where the \mathbf{P}^D -th phase sub-block is located

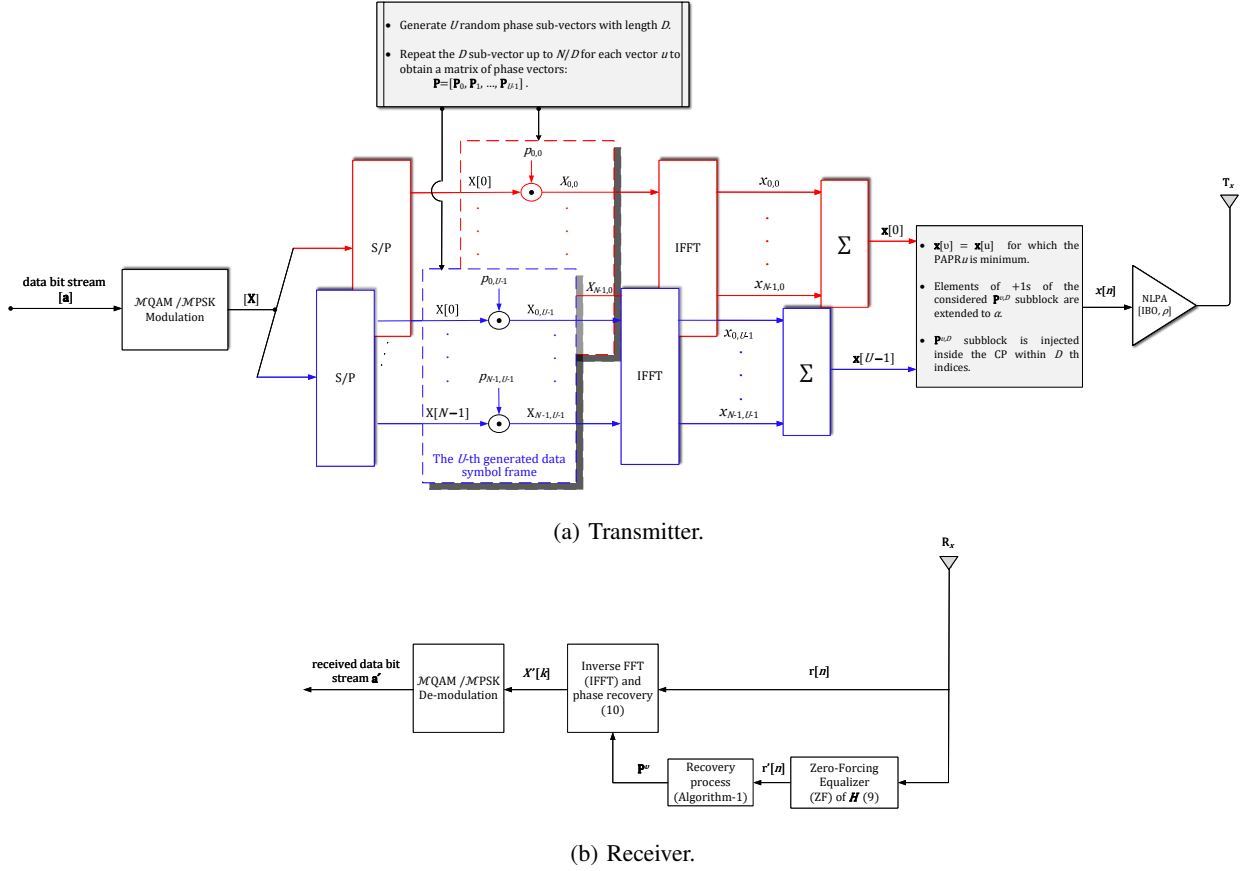


Fig. 1. Block diagram of the proposal at: (a) Transmitter and (b) Receiver.

inside the CP. Therefore, the length of this equalizer can be shorter. In other words, instead of operating the ZF equalizer for all $N + N_c$ indices, it is sufficient to implement the process only for the indices $[-N_c, -N_c + 1, \dots, -1]$ leading to a lower computational complexity, taking into account that a trade off between the computational complexity and the system performance is substantial. Based on that, the resultant converted subsequence can be expressed as

$$\mathbf{r}^D = \mathbf{g}^{ZF} \cdot \mathbf{r}. \quad (9)$$

To define the desired phase sub-block $\mathbf{P}^{v,D}$, the resultant vector \mathbf{r}^D is compared to the threshold $|\alpha|$, where $\alpha = \mathbf{E}\{|r[n]|\} + j\mathbf{E}\{|r[n]|\}$ as represented in Algorithm 1.

Algorithm 1 Proposed Algorithm

- 1: Input: index D for $0 \ll D \ll N_c - 1$, $\mathbf{r}' = |\mathbf{r}^D|$, $|\alpha|$.
- 2: **for** $i = n + 1 : n + D$ **do**
- 3: **if** $|r'(i)| \geq |\alpha|$ **then**, $p^v(i) = 1$,
- 4: **if** $|r'(i)| < |\alpha|$ **then**, $p^v(i) = -1$
- 5: **end if**
- 6: **end if**
- 7: **end for**
- 8: $\mathbf{P}^{v,D} = \text{repmat}(\mathbf{P}^v, 1, \frac{N}{D})$

its original phases after operations of fast Fourier transform (FFT), channel effect removal and demodulation as follows

$$X'[k] = \frac{FFT[r[n] \mid 0 \leq n \leq N-1]}{\mathbf{P}^{v,D}[k]}, \quad \text{for } 0 \leq k \leq N-1. \quad (10)$$

III. NUMERICAL RESULTS AND DISCUSSIONS

In the proposed method the following assumptions have been considered for simulation purposes:

- 1) All N subcarriers of all OFDM samples are active.
- 2) The matrix of multi-path fading channel \mathbf{h} is perfectly known at the receiver.
- 3) The threshold value α is equivalent to the mean value of the transmitted OFDM frame at both the transmitter and receiver, and it is adjusted as a complex component, i.e. $\alpha_t = \mathbf{E}\{|x[n]|\} + j\mathbf{E}\{|x[n]|\}$ and $\alpha_r = \mathbf{E}\{|r[n]|\} + j\mathbf{E}\{|r[n]|\}$, where α_t and α_r indicate the transmission and reception threshold value, respectively.
- 4) The index D has been reserved to inject the sub-vector \mathbf{P}^v inside the cyclic prefix block N_c , where $D \ll N_c$.
- 5) The index of D is known perfectly at the transmitter and receiver.
- 6) Effects of ISI and ICI are completely overcome, where ISI is due to the OFDM post-transient phase leading to an OFDM symbols overlap and ICI is due to the pre-transient phase of

Last but not least, the received signal is converted to

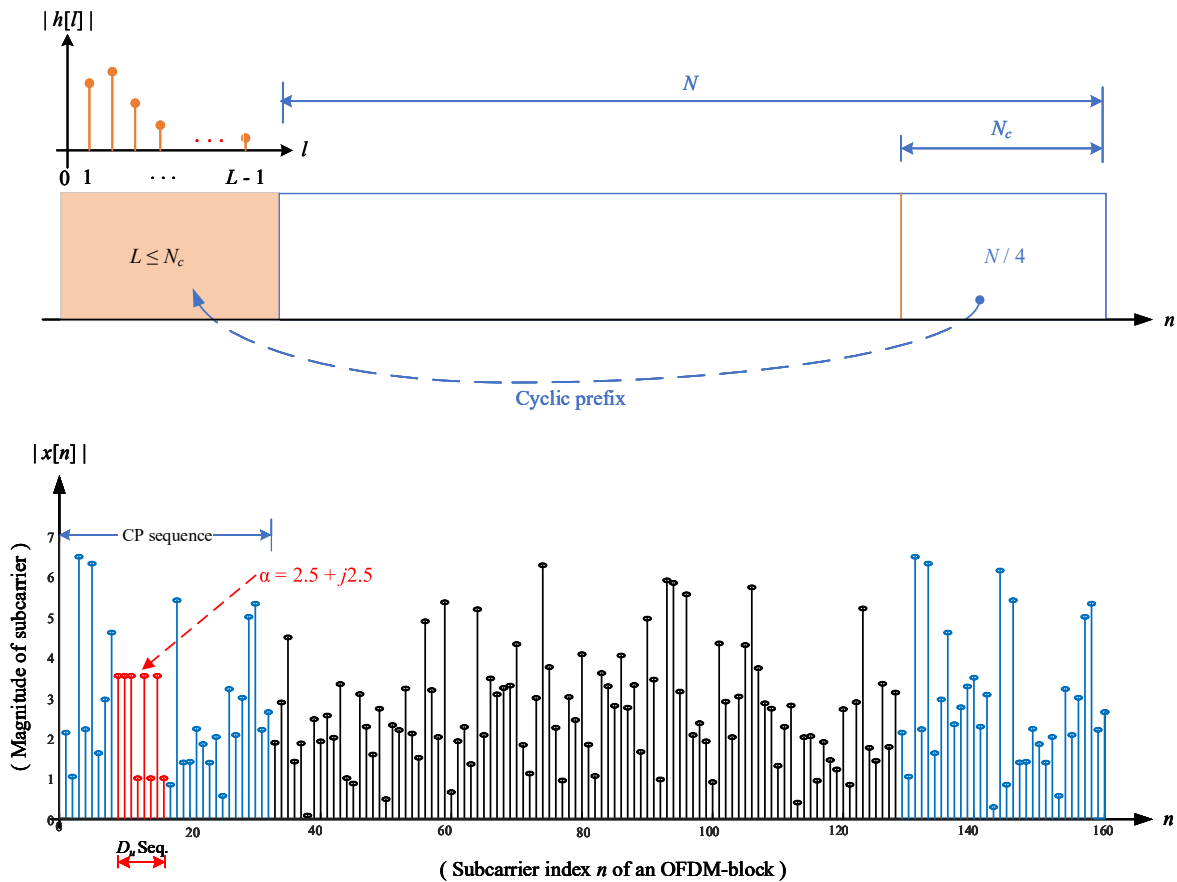


Fig. 2. Block diagram of the cyclic prefix and an example that explains the concept of the proposal at $N = 128$ subcarriers, $\mathbf{P}^{v,D} = 8$ samples and a threshold $\alpha = 2.5 + j2.5$.

OFDM symbols.

7) The Solid-State Power Amplifier (SSPA) of C. Rapp [25] was implemented in this proposal with the following output amplitude and phase models:

$$G[x(n)] = \frac{v|x(n)|}{\left[1 + \left(\frac{v|x(n)|}{A_0}\right)^{2\rho}\right]^{\frac{1}{2\rho}}}, \quad \text{and} \quad \Phi[\mathbf{x}] \approx 0, \quad (11)$$

where, $v = 1$ is the small gain, $A_0 = vA_s$ and $A_s = \sqrt{IBO \cdot \mathbf{E}\{|x[n]|^2\}}$ is the saturation amplitude with different linear values of Input-Back-Off (IBO), and $\rho = 3$ is the knee factor.

8) Inputs factors are identified in Table-I.

A. CCDF-PAPR Performance

Generally, the CCDF of the PAPR reduction is used to evaluate the characteristic of a represented scheme in comparison to either the non-PAPR, the theoretical, or another PAPR reduction technique curves. Theoretically, the complementary commutative-distribution function (CCDF) of the $PAPR^v$ is defined as the probability that the lowest $PAPR^v$ exceeds a given threshold $PAPR_0$. When jointly applying U trails for

TABLE I
INPUT FACTORS OF THE PROPOSED IES-SLM-CP MODEL.

Input factor	Abbreviation	Value
No. of subcarrier/frame	N	64, 128, 256
size of constellation	M -QAM	4, 16, 64, 128
No. of candidate phase sub-block	U	4
length (index) of candidate sub-block	D	4, 8, 16
input-back-off (dB)	IBO	3, 5, 7
length of cyclic prefix	N_c	$\frac{N}{4}$
number of paths of Rayleigh channel	L	$\frac{4N}{8}$
Threshold value at [+1]s	α	$\alpha = \beta + j\gamma$

the OFDM symbols, and from (2), the following expression can be approximated:

$$Pr\{PAPR_v > PAPR_0\} = \left(1 - (1 - e^{-PAPR_0})^{\epsilon N}\right)^{U+1}, \quad (12)$$

where ϵ is a practical approximation [26]. From this point, Fig.3 illustrates characteristics of the proposed IES-SLM-CP with respect to the non-PAPR reduction and theoretical CCDF-PAPR performances. The figure shows an improvement in the CCDF-PAPR reduction of the proposal as long as the

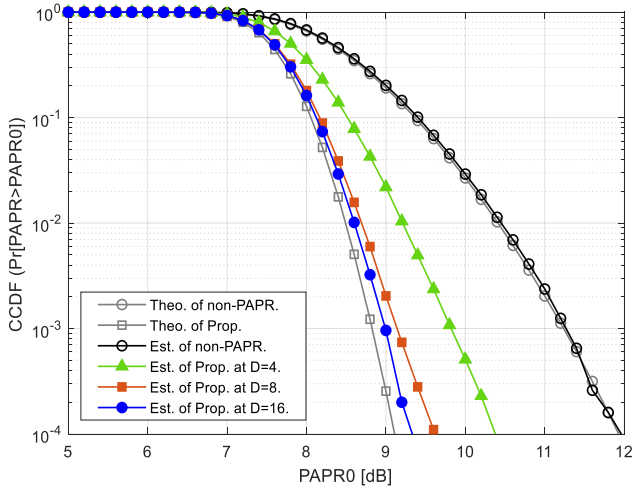


Fig. 3. CCDF-PAPR performance for OFDM frames at different number of random phase elements/sub-block \mathbf{P}^D where $U = 4$ candidate phase vectors, with $N = 128$ subcarriers/frame, $\text{IBO} = 5\text{dB}$, and 16QAM modulation.

length of the sub-vector D increases. The reason behind this improvement is the reduction of similarity between the generated sub-vectors $\mathbf{P}^{u,D}$. Consequently, the correlation between each designed phase block \mathbf{P}^u and another becomes less, with increasing the duration D , so that the desired PAPR reduction level is achieved. However, a trade off between this development and the system performance (BER/SIER) must be taken into account, as will be discussed in the next subsection.

B. Bit and Side-Information Error Rate (BER/SIER) Performances

In this section, we study the attitude of the proposed method from the perspective of the BER and SIER in comparison to the theoretical performance of the transmitted MQAM OFDM signal. In the best of circumstances, since the main source affecting the performance of any wireless communication system is the fading originating from the multipath channel, this theoretical performance will be considered as a reference for the proposed system performance measure. Knowing that there are other sources that affect the performance of the communication system (in relation to our research field), for example, but not limited to, the effect of a non-linear power amplifier, which is controlled by the input-back-off (IBO) of the PA. In addition, depending on the concept of the proposed IES-SLM-CP, there will be an impact on the system performance (BER) arising from the process of restoring and constructing the desired side information, at the receiver side. Particularly, the recovery error, which is also referred to as side information error rate (SIER), is produced by the length, location, and value of the injected phase subblock $\mathbf{P}^{v,D}$ when exposed to the direct influence of a channel fading, which in turn is reflected in the overall system performance (BER). Notice that such a phase sub block is highly sensitive of channel effect because it has been injected during the CP, which was initially designed to absorb the effect of multi-path fading channel. Based on that, results of Fig.4 illustrate the BER performances for different sizes of QAM constellation, that is 16QAM, 64QAM, and 128QAM, where $N = 256$

subcarriers/frame, $\text{IBO} = 7\text{dB}$, $D = 4$ elements/sub-block, and $U = 4$ candidate phase block. As can be noticed from the figure that the performance is identical to theoretical for each MQAM constellation. On the other side, based on the SIER, Fig.5 shows characteristics of SIER with respect to SNR, where the SIE is accounted for the entire side information sub-block $\mathbf{P}^{u,D}$ at any occurred error of an element. Accordingly, the best character is illustrated at the high MQAM, that is 128QAM. In short, the higher the average energy of MQAM constellation points, the higher α value inside the SI, which leads to a comparable differences between SI elements and this helps to elicit and reconstruct elements of SI $\mathbf{P}^{v,D}$ (taking into account that the $+1\text{s}$ elements inside the SI sub-block were extended to α , while the -1s elements were unchanged). In addition to that, Fig.6 represents the SIER of 4QAM, 16QAM, 64QAM, and 128QAM with respect to the length of equalizer with low and high SNR values, that is $\text{SNR} = 5$ and 35dB , at $N = 64$ subcarrier/frame, $\text{IBO} = 3\text{dB}$, $D = 4$ elements/sub-block. Here, it is remarkable that the high SNR improves the SI performance, which will reflect in the BER performance as well. This fact is true for all MQAM formats except 4QAM which shows bad SIER performance even when increase SNR to the highest level. This is because of the approximate equivalence between the mean energy of 4QAM and the α value inside the SI, which causes difficulty in extracting the latter and errors in its reconstructed elements.

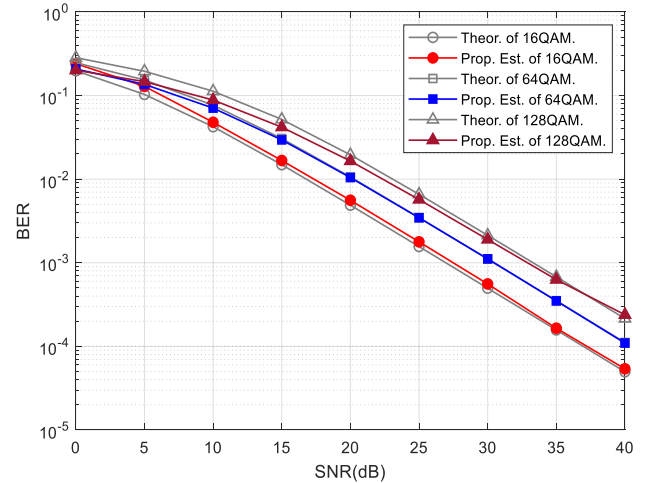


Fig. 4. Comparisons of BER performance of different sizes of MQAM constellation with $N = 256$ subcarrier/frame, $D = 4$ elements/sub-block, $U = 4$ candidate phase block, and $\text{IBO} = 7\text{dB}$.

Moreover, from Fig.7, it is observed that performance of both 16QAM and 64QAM is improved when increasing the level of linearity of the power amplifier, that is at 7dB input-back-off, where $N = 256$ subcarrier/frame, $D = 4$ candidate elements/sub-block, and $U = 4$ overall candidate phase blocks. In other words, the performance becomes worse at low IBO (i.e. $\text{IBO} = 5\text{dB}$) due to the nature of the non-linear PA where a higher number of OFDM peaks are clipped, and thus a higher BER is introduced.

Last but not least, when increasing the length of the candidate phase sub-block D , it means that the side information is located, in somehow, corresponding to the maximum channel effect. In this case, rising energy of transmitted signal (i.e.

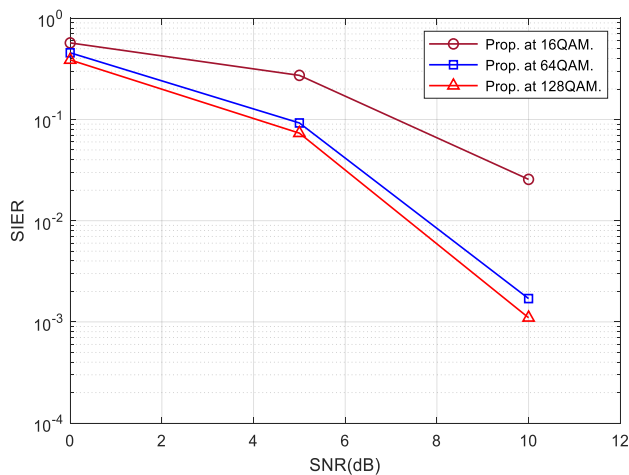


Fig. 5. Comparisons of SIER performance of different sizes of MQAM constellation with $N = 256$ subcarrier/frame, $D = 4$ elements/subblock, $U = 4$ candidate phase block, and $IBO = 3$ dB.

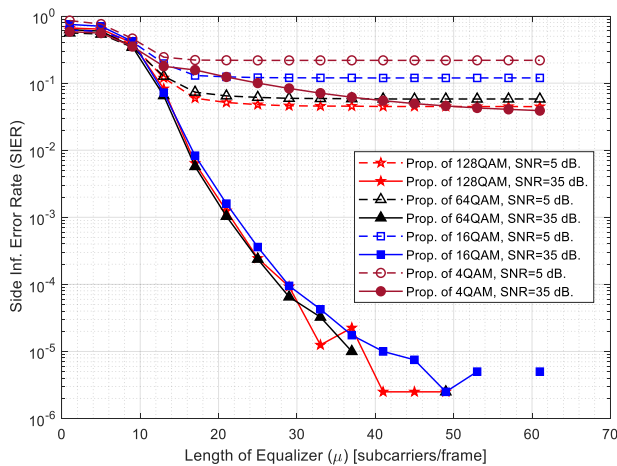


Fig. 6. Comparisons of SIER at different size of constellation mapping MQAM and SNR (dB) for $N = 64$ subcarrier/frame, $D = 4$ elements/subblock, $U = 4$ candidate phase sequence, $IBO = 3$ dB.

SNR) or the value of α will not keep the transmitted phase sub-vector $\mathbf{P}^{v,D}$ safe against channel effect. Especially since this generated phase sub-vector is located inside the cyclic prefix period, which was essentially designed to absorb the channel effects, as depicted in Fig.8 which represents the impact of different length of sub-block D , on both (a) BER and (b) SIER performances, at 16QAM, $N = 64$ subcarrier/block, $IBO = 5$ dB, and $U = 4$ phase blocks. Noting that the given factor Δ was multiplied by the measured α such that the new value of α is equivalent to $\Delta\alpha$ for study purposes, while the Δ is given any integer number. Consequently, these figures show that the increase in the value of Δ (i.e. at $\Delta = 3$) degrades further system performance BER, despite the improvement obtained in the SIER. This means that the increase in the length of sub-block $\mathbf{P}^{v,D}$ reached the maximum channel fading region. As a result, a distorted side information and, in turn, BER is obtained. This concept is confirmed by the obtained development in the BER performance when rising the length of the OFDM block N to 128 subcarrier/frame, such that the length of CP has been increased as well, leading to protecting the side information stored inside CP from the effect of the

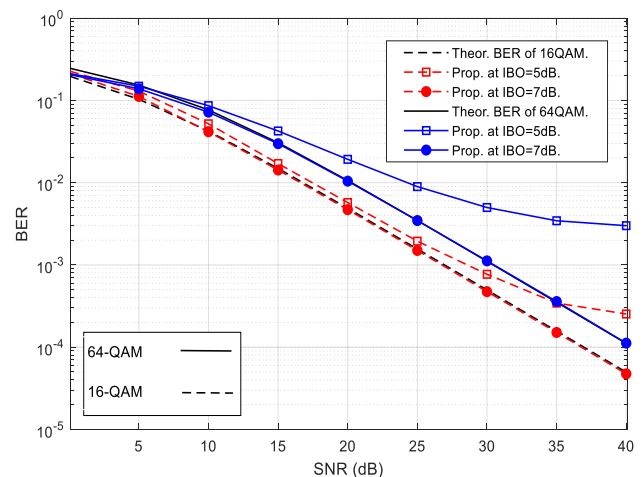


Fig. 7. BER of a 256 subcarriers OFDM symbol for 16QAM and 64QAM at different level of IBO, $U = 4$ candidate phase sequences and $D = 4$ phase subsequence.

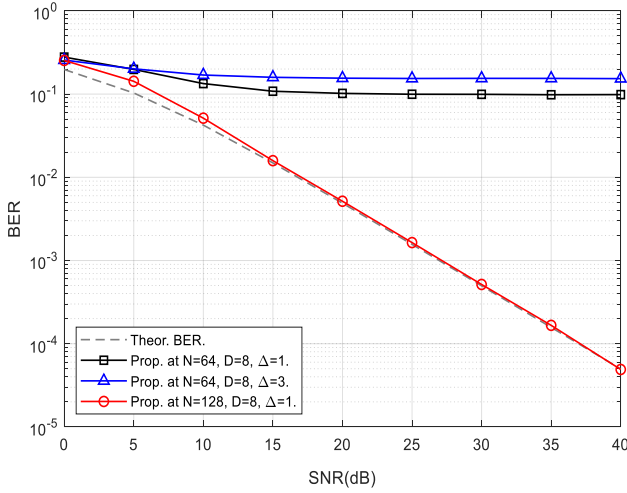
multipath fading channel. Therefore, as mentioned previously, a trade off between the PAPR reduction level and BER performance is necessary to consider the appropriate length of D . To discuss this phenomenon, a short analytical discussion of ISI/ICI at a specific element of phase subsequence $p^{v,D} = \alpha$ is provided as follows. Hence, a modified formula of (5) can be represented, after removing effect of AWGN noise, as: $r[n] = h_0x_n + \sum_{l=1}^{L-1} h_lx_{n-l}$ where the component h_0x_n indicates the line of sight signal (LOS) which is considered as a desired signal S_n . While the rest component represents the inter-symbol-interference I_n . Because our interest is at the side information elements inside the CP duration, specifically at the considered phase element $p^{v,D} = \alpha$ which is located at index n_d , where $n_d \in \{D|N_c \ll D \ll 0\}$, hence the signal-to-interference power ratio (SIPR) can be expressed as;

$$SIPR = \frac{E[|S_{n_d}|^2]}{E[|I_{n_d}|^2]} = \frac{|\alpha|^2|h_0|^2}{\left(\sum_{l=1}^{L-1}|h_l|^2\right)(|x_{n \neq n_d}|^2; |\alpha|^2)}, \quad (13)$$

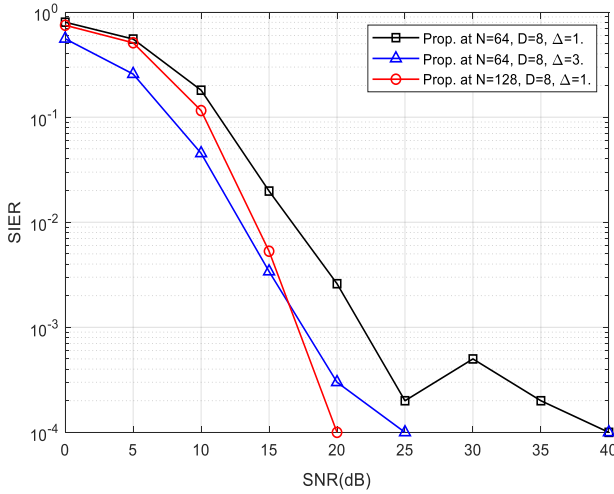
where $(|x_{n \neq n_d}|^2; |\alpha|^2)$ indicates both the average energy per symbol of MQAM constellation and the magnitude of injected (α) at a specific subcarriers surround n_d due to the convolution operation. Based on that, it is possible to improve the side information error caused by the multipath fading channel, and hence the BER performance, by mainly increasing the length of CP N_c , at a certain D , to take this side information away from the maximum impact of the channel. On the other hand, rising the value of α will not improve the SIPR ratio because the modified α value in the numerator will be equivalent to that in the denominator of (13), so this update is almost intangible. This fact is promoted by the results illustrated in Fig.8, which was previously explained. Accordingly, BER performance at $N = 128$ is improved dramatically because the SIPR ratio is increased, even though Δ is effectiveness, that is $\Delta = 1$.

C. Computational Complexity and Increase Energy

It is worth mentioning that the previous results have been obtained when operating the equalizer in (9) for the entire dimensions of the matrix, i.e. $(N + L) \times (N \cdot N_c)$, which means



(a) BER.



(b) SIERRA.

Fig. 8. Comparisons of: (a) BER and (b) SIERRA, at different length of OFDM block N and extension factor Δ when increasing length of phase sub-block to $D = 8$ for 16QAM, $U = 4$ candidate phase block, and IBO= 5.

a full computational complexity of the recovery. However, when limiting the operation of equalizer only to dimensions $\mu_1 \times \mu_2$, the recovery computational complexity is reduced dramatically, where μ_i can take any integer value such that $\mu_1 < (N + L)$ and $\mu_2 < (N \cdot N_c)$ (say $\mu_1 = \mu_2 = N_c$ or less), whereas the system performance is negatively affected by this modification. This negative result can be remedied by raising the value of α to $(\Delta\alpha)$ with $\Delta > 1$, as illustrated in Fig.9. Knowing that the factor μ_i was assumed, to reduce the equalizer matrix dimension, for testing and simulation purposes only. It must be taken into account that the reduction in the dimensions of equalizer must be limited to a certain level for the possibility of recovering all side information elements. Also, the extension value of α should be considered carefully to avoid effect of saturation level of the PA. Despite that, the source of the computational complexity is mainly from discrete Fourier transform and its inverse operations (IDFT at the transmitter and DFT at the receiver), however, it is important to consider the computational complexity caused by the implemented extra operations of the modified system, at

TABLE II
COMPARISONS OF COMPUTATIONAL COMPLEXITY.

Proposals	Multiplications Complexity	Summation Complexity
Proposed IES-SLM-CP	$D + N_c + N \left(\frac{(U+1)N}{2} \right) \log_2 N + \left(\frac{N}{2} \right) \log_2 N.$	$(Nc - 1) + (U + 1)N \log_2 N + N \log_2 N.$
IQ-SLM ¹	$Ul + N(12 + 3U) \left(\frac{(U+1)N}{2} \right) \log_2 N + \left(\frac{N}{2} \right) \log_2 N.$	$8N(U + 1) + (U + 1)N \log_2 N + N \log_2 N.$
I-SLM ²	$M \frac{N}{2} \log_2 N + N^2 (M + 3).$	$MN \log_2 N + 2(N - 1)M.$
Conv-PTS ³	$(V + 1) \frac{N}{2} \log_2 N + (Q + 2) \frac{N}{2}$	$(V + 1)N \log_2 N + U(V - 1)N + 2QN.$

¹ l is referred to the number of candidate sub-vector in [11].

² M is referred to the number of iterations in [12].

³ Q is referred to the size of QAM constellation in [20].

both transmitter and receiver. In this section, we will consider the schemes of SLM/PTS on which the generated phase vectors \mathbf{P}^u are approximately the same. Therefore, same input parameters have been considered for all represented methods in order to obtain a fair and realistic comparison, that are the OFDM N subcarrier/frame, U candidate phase vector, D phase sub-vector (for this proposal), $l = \frac{N}{U}$ phase sub-vectors for IQ-SLM, M number of iterations of I-SLM, and Q size of constellation of conventional PTS. Accordingly, Table II represents computational complexity comparisons between the proposed IES-SLM-CP scheme and the IQ-SLM [11], I-SLM [12] and Conv-PTS [20] proposals.

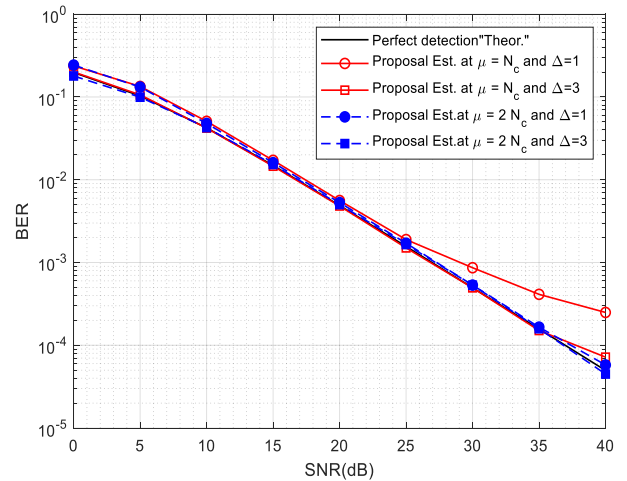
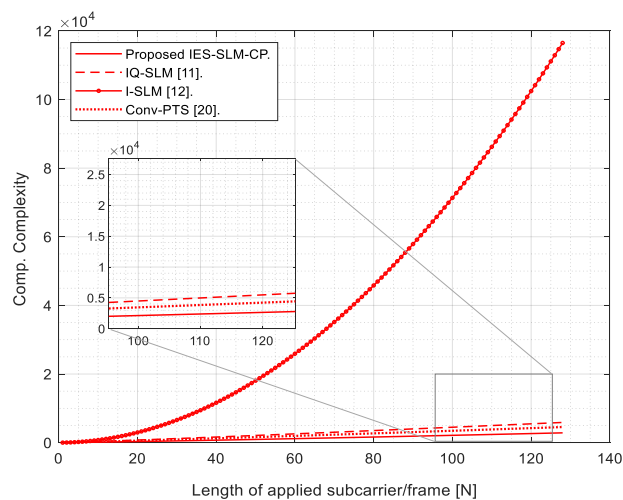
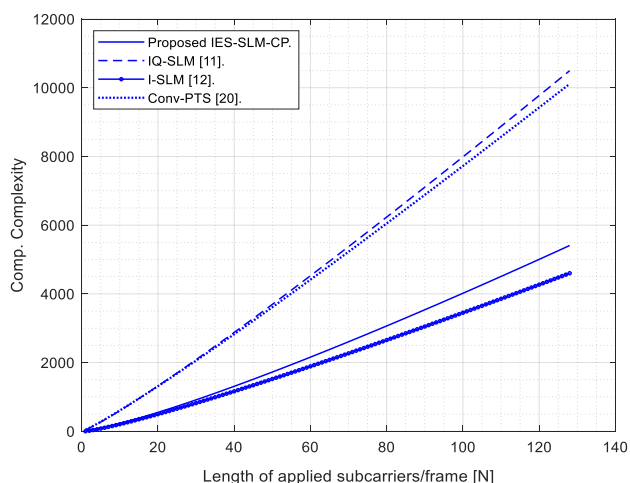


Fig. 9. BER of a subcarriers OFDM symbol with length $N = 128$ for 16-QAM at different values of Δ (i.e. different short lengths of equalizer), $D = 4$ elements/sub-block, $U = 4$ candidate phase block and IBO= 5dB.

Bearing in mind that the extended elements inside D proposed factor are located at the positive elements only (i.e. at $+1s$). However, to study the computational complexity, the worst case is considered which means that all elements inside parameter D have been supposed to be extended (i.e. multiplied by factor α). In addition to that, the recovery length can be operated below N_c , while it considered here to be equal to N_c to study the computational complexity characteristic. Consequently, Fig.10 demonstrates the compu-



(a) Multiplication operations complexity.



(b) Summation operations complexity.

Fig. 10. Comparisons of computational complexity of: a) Multiplications operations and b) Summations operations, versus length of OFDM transmitted block N (based on Table-II).

tational complexity (based on Table-II), of a) Multiplication operations and b) Summation operations, versus length of N subcarrier/frame at $D = 4$ elements/sub-block, $l = 4$ sub-vector, $M = 4$ iterations and $Q = 16$ size of QAM constellation. Fig.10a shows that the proposed IES-SLM-CP provides the lowest multiplication computational complexity over other represented methods, while I-SLM scheme, in Fig.10b, won over others proposals and the proposed IES-SLM-CP came next, however its summation computational complexity still comparable.

IV. CONCLUSIONS

In this paper, a new method which is referred to as injected and extended short SLM to and from the CP (IES-SLM-CP) is represented. This proposal is able to reduce the high OFDM peaks-to-average power ratio to an acceptable level while the desired phase vector can be recovered blindly. The concept of this proposal depends on the benefits of CP period by injecting a very short sample of the desired SLM sub-vector inside the CP, where, mostly, the minimum impact of the multipath fading channel on this location is weak. As a result, this

proposal represents an acceptable performances of both PAPR and BER at low computational complexity comparing to other samples distortionless techniques which were discussed in this paper. As a future work, we look forward to considering other aspects of efficiency and performance standards such as the block error rate (BLER) and CP length efficiency in the event that the proposed system is an encrypted system.

ACKNOWLEDGMENT

This paper has been funded by Researchers Supporting Project number (RSP2022R484), King Saud University, Riyadh, Saudi Arabia.

REFERENCES

- [1] S. A. Fathy, M. Ibrahim, S. El-Agooz and H. El-Hennawy, "Low-Complexity SLM PAPR Reduction Approach for UPMC Systems," in *IEEE Access*, vol. 8, pp. 68021-68029, 2020. doi: 10.1109/ACCESS.2020.2982646.
- [2] S. P. Valluri, V. Kishore and V. M. Vakamulla, "A New Selective Mapping Scheme for Visible Light Systems," in *IEEE Access*, vol. 8, pp. 18087-18096, 2020. doi: 10.1109/ACCESS.2020.2968344
- [3] Y. A. Al-Jawhar, K. N. Ramli, M.A. Taher, N. S. M. Shah, S. A. Mostafa and B. A. Khalaf, "Improving PAPR performance of filtered OFDM for 5G communications using PTS," *ETRI Journal*, vol. 43: pp. 209-220, 2021. doi.org/10.4218/etrij.2019-0358
- [4] A. Mohammed, T. Ismail, A. Nassar and H. Mostafa, "A Novel Companding Technique to Reduce High Peak to Average Power Ratio in OFDM Systems," in *IEEE Access*, vol. 9, pp. 35217-35228, 2021. doi: 10.1109/ACCESS.2021.3062820.
- [5] F. Sandoval, G. Poitau and F. Gagnon, "On Optimizing the PAPR of OFDM Signals With Coding, Companding, and MIMO," in *IEEE Access*, vol. 7, pp. 24132-24139, 2019. doi: 10.1109/ACCESS.2019.2899965.
- [6] S. Gokceli, I. Peruga, E. Tirola, K. Pajukoski, T. Riihonen and M. Valkama, "Novel Tone Reservation Method for DFT-s-OFDM," in *IEEE Wireless Communications Letters*, vol. 10, no. 10, pp 2130-2134, Oct. 2021. doi: 10.1109/LWC.2021.3094887.
- [7] B. Bakkas, R. Benkhrouya, I. Chana, and H. Ben-Azza, "Palm Date Leaf Clipping: A New Method to Reduce PAPR in OFDM Systems," *Information*, vol. 11, no. 4, p. 190, Apr. 2020. doi: 10.3390/info11040190.
- [8] S. Gokceli et al., "Novel Iterative Clipping and Error Filtering Methods for Efficient PAPR Reduction in 5G and Beyond," in *IEEE Open Journal of the Communications Society*, vol. 2, pp. 48-66, 2021, doi: 10.1109/OJCOMS.2020.3043598.
- [9] X. Wang, N. Jin and J. Wei, "A Model-Driven DL Algorithm for PAPR Reduction in OFDM System," in *IEEE Communications Letters*, vol. 25, no. 7, pp. 2270-2274, July 2021. doi: 10.1109/LCOMM.2021.3076605.
- [10] X. Lu, Y. Shi, W. Li, J. Lei and Z. Pan, "A Joint Physical Layer Encryption and PAPR Reduction Scheme Based on Polar Codes and Chaotic Sequences in OFDM System," in *IEEE Access*, vol. 7, pp. 73036-73045, 2019. doi: 10.1109/ACCESS.2019.2919598.
- [11] M. I. Al-Rayif, H. E. Seleem, A. M. Ragheb, and S. A. Alshebeili, "PAPR Reduction in UPMC for 5G Cellular Systems," *Electronics*, vol. 9, no. 9, p. 1404, Aug. 2020. doi: 10.3390/electronics9091404.
- [12] M. I. Al-Rayif, H. Seleem, A. Ragheb and S. Alshebeili, "A Novel Iterative-SLM Algorithm for PAPR Reduction in 5G Mobile Fronthaul Architecture," in *IEEE Photonics Journal*, vol. 11, no. 1, pp. 1-12, Feb. 2019, Art no. 7201112. doi: 10.1109/JPHOT.2019.2894986.
- [13] S. Thota, Y. Kamatham and C. S. Paidimarry, "Analysis of Hybrid PAPR Reduction Methods of OFDM Signal for HPA Models in Wireless Communications," in *IEEE Access*, vol. 8, pp. 22780-22791, 2020. doi: 10.1109/ACCESS.2020.2970022.
- [14] J. Hou, W. Wang, Y. Zhang, X. Liu and Y. Xie, "Multi-Objective Quantum Inspired Evolutionary SLM Scheme for PAPR Reduction in Multi-Carrier Modulation," in *IEEE Access*, vol. 8, pp. 26022-26029, 2020. doi: 10.1109/ACCESS.2020.2971633.
- [15] H. -Y. Liang, "Selective Mapping Technique Based on an Adaptive Phase-Generation Mechanism to Reduce Peak-to-Average Power Ratio in Orthogonal Frequency Division Multiplexing Systems," in *IEEE Access*, vol. 7, pp. 96712-96718, 2019. doi: 10.1109/ACCESS.2019.2929769.

- [16] B. Cai, A. Liu and X. Liang, "Low-Complexity Selective Mapping Methods for Multicarrier Faster-Than-Nyquist Signaling," in *IEEE Access*, vol. 8, pp. 31420-31431, 2020. doi: 10.1109/ACCESS.2020.2973394.
- [17] M. F. Haroun and T. A. Gulliver, "Secure OFDM with Peak-to-Average Power Ratio Reduction Using the Spectral Phase of Chaotic Signals," *Entropy*, vol. 23, no. 11, p. 1380, Oct. 2021. doi: 10.3390/e23111380.
- [18] S. Simsir and N. Taspinar, "A novel discrete cuckoo search algorithm-based selective mapping technique to minimize the peak-to-average power ratio of universal filtered multicarrier signal," *International Journal of Communication Systems*, vol. 33, no. 18, p. e4640, 2020. doi.org/10.1002/dac.4640
- [19] Y. M. Al-Moliki, M. T. Alresheedi and Y. Al-Harhi, "Secret Key Generation Protocol for Optical OFDM Systems in Indoor VLC Networks," in *IEEE Photonics Journal*, vol. 9, no. 2, pp. 1-15, April 2017, Art no. 7901915. doi: 10.1109/JPHOT.2017.2667400.
- [20] H. -S. Joo, K. -H. Kim, J. -S. No and D. -J. Shin, "New PTS Schemes for PAPR Reduction of OFDM Signals Without Side Information," in *IEEE Transactions on Broadcasting*, vol. 63, no. 3, pp. 562-570, Sept. 2017. doi: 10.1109/TBC.2017.2711141.
- [21] L. Samara, A. O. Alabassi, R. Hamila and N. Al-Dhahir, "Sparse Equalizers for OFDM Signals With Insufficient Cyclic Prefix," in *IEEE Access*, vol. 6, pp. 11076-11085, 2018. doi: 10.1109/ACCESS.2018.2795596.
- [22] P. Beckmann, "Rayleigh distribution and its generalizations," *Journal of Research of the National Bureau of Standards, Section D: Radio Science*, vol. 68D, no. 9, pp. 927-932, Sept. 1964. doi.org/10.6028/jres.068d.092
- [23] Xiaoyi Tang, M. . -S. Alouini and A. J. Goldsmith, "Effect of channel estimation error on M-QAM BER performance in Rayleigh fading," in *IEEE Transactions on Communications*, vol. 47, no. 12, pp. 1856-1864, Dec. 1999. doi: 10.1109/26.809706.
- [24] C. Wang, E. K. S. Au, R. D. Murch, W. H. Mow, R. S. Cheng and V. Lau, "On the Performance of the MIMO Zero-Forcing Receiver in the Presence of Channel Estimation Error," in *IEEE Transactions on Wireless Communications*, vol. 6, no. 3, pp. 805-810, March 2007. doi: 10.1109/TWC.2007.05384.
- [25] C. Rapp, "Effects of HPA-nonlinearity on a 4-DPSK/OFDM-signal for a digital sound broadcasting signal", in *ESA Special Publication*, 1991, vol. 332, pp. 179-184.
- [26] R. van Nee and A. de Wild, "Reducing the peak-to-average power ratio of OFDM," *VTC '98. 48th IEEE Vehicular Technology Conference. Pathway to Global Wireless Revolution (Cat. No.98CH36151)*, 1998, pp. 2072-2076, vol.3. doi: 10.1109/VETEC.1998.686121.



Mohammed I. Al-Rayif holds a bachelor's degree in Electrical Engineering from King Saud University, Riyadh, Saudi Arabia in the field of Electrical Engineering. He received his MSc and PhD degrees from Newcastle University, UK in 2006 and 2010 respectively in Communications and Signal Processing. From 1998 to 2014, he held several positions in the General Directorate of Border Guards in the Ministry of Interior in the Kingdom of Saudi Arabia, including for example the Head of Wired / Wireless Systems Department (2000-2003) and Director of Communications Systems in the Border Guards (2011-2013). He served as Chairman of the Electrical Engineering Department and Vice Dean of the College of Engineering at King Khalid University in Ahab (2014-2017). During the period 2018-2019, he was a collaborating faculty member with the Department of Applied Electrical Engineering, Al-Muzahimiyah branch, King Saud University. Mohamed Al-Rayif has been working since 2019 as an associate professor in the Department of Applied Electrical Engineering. His research interests include OFDM and MIMO systems, artificial intelligence techniques, mm wave communications. Mohammed Al-Rayif has contributed his research publications to many prestigious international journals and conferences.